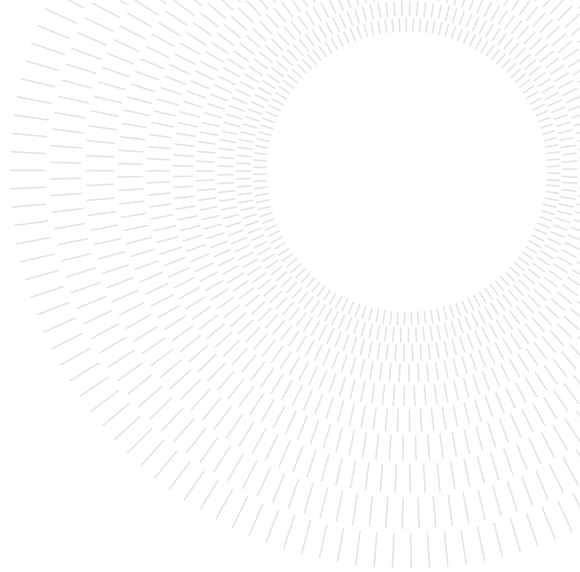




POLITECNICO
MILANO 1863

SCUOLA DI INGEGNERIA INDUSTRIALE
E DELL'INFORMAZIONE



BAYESIAN STATISTICS PROJECT FINAL REPORT

CLUSTERING WEEKLY DATA OF ONE YEAR OF PM2.5 DATA

LAUREA MAGISTRALE IN MATHEMATICAL ENGINEERING

Authors: BORRINI ELISA, CARBONARA FILIPPO, CEFALONI BENEDETTA, ETTEL DINA SOPHIE, GRIGNANI ALESSANDRO, WOLF FLORIAN

Advisors: MICHELA FRIGERI, ALESSANDRO CARMINATI

Academic year: 2023-2024

1. Introduction

Air Quality Challenges in Lombardy, Italy: Air pollution, a critical environmental concern, poses significant risks to human health and the ecosystem. The Lombardy region in Italy faces significant air pollution challenges, ranking among the most polluted areas in Europe. This issue arises from factors such as limited air circulation and high emission levels.

Among the various pollutants, particulate matter with a diameter of 2.5 micrometers or smaller (PM2.5) has emerged as a key focus due to its potential for adverse health effects. PM2.5 consists of tiny particles suspended in the air, originating from diverse sources such as vehicle emissions, industrial activities, and natural processes.

Understanding the temporal patterns of PM2.5 levels is crucial for identifying trends, potential sources, and developing effective pollution control strategies. Clustering techniques will be employed to categorize weeks with similar PM2.5 concentration profiles, providing insights into the underlying patterns and contributing factors. In order to do this, our project analyzes a dataset spanning the years 2016 to 2021 [Rod+23], collecting daily values of air quality, weather conditions, emissions, livestock, and land and soil use. Pollutant data are sourced from the European Environmental Agency and the Lombardy Regional Environment Protection Agency, Weather and emissions data are obtained from the European Copernicus program, livestock data from the Italian zootechnical registry, and land and soil use data from the CORINE Land Cover project. The project focuses on analyzing and clustering weekly data of PM2.5 concentrations over the course of one year (2019), trying to assess the impact of agriculture on air quality in the selected area through statistical techniques and highlighting the relationship between the livestock sector and the air pollutant concentrations.

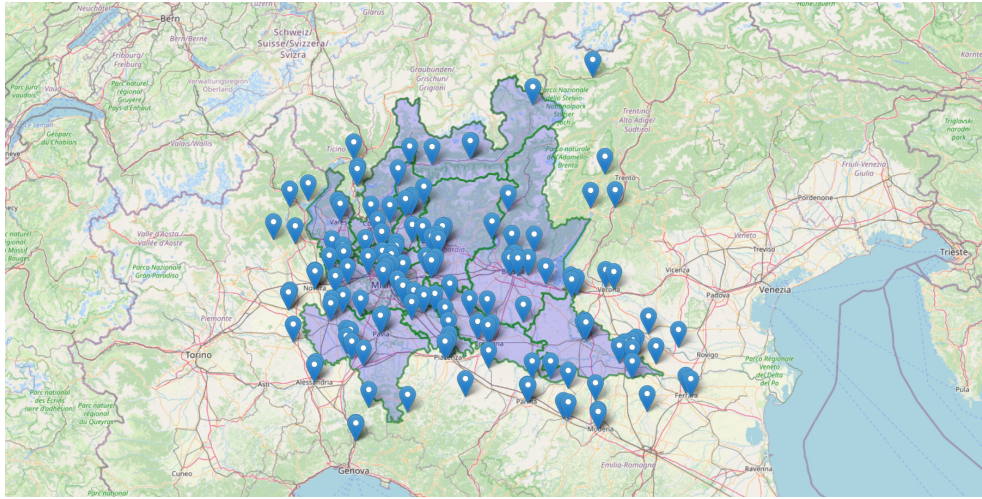


Figure 1: Buffered Area around Lombardy Region

2. Data and Covariates

The Agrimonia dataset integrates satellite data, model output, and in-situ measurements sourced from national and international agencies, each with varying spatial and temporal resolutions.

Source Data Overview: The dataset encompasses five key dimensions: air quality (AQ), weather and climate (WE), pollutant emissions (EM), livestock (LI), and land and soil characteristics (LA). Given the applicability of geostatistical methods in leveraging neighboring territory information for enhanced predictive capability near borders, a 0.3° buffer is applied around the Lombardy region, intersecting with several adjacent regions (Figure 1).

Causes and sources related to the emissions: Particulate matter with a diameter of 2.5 micrometers or smaller originates from various anthropogenic and natural sources. Among the main causes related to the release of significant amounts of PM2.5 into the atmosphere, we can mention intensive livestock farming, as well as combustion processes, including those from vehicles and industrial activities. Moreover, analyzing the provided dataset, it has emerged that one crucial variable influencing PM2.5 concentrations is the Boundary Layer Height (BLH) Max which represents the maximum depth of air next to the Earth's surface that is most affected by the resistance to the transfer of momentum, heat, or moisture across the surface.

Main Problems Associated with PM2.5: In order to understand the relevance of the analysis developed in this project, it is important to focus on the problems and the risks associated with high concentrations of PM2.5

- **Long Residence Time in the Atmosphere:** PM2.5 particles have an extended residence time in the atmosphere, leading to widespread dispersion and potential long-range transport. This characteristic contributes to the global distribution of PM2.5 and its diverse environmental impacts.
- **Health Impact:** Due to their small size, PM2.5 particles can penetrate deep into the human respiratory system, reaching the lungs and even entering the bloodstream. Prolonged exposure to elevated levels of PM2.5 is associated with various respiratory and cardiovascular diseases, posing a significant public health concern.
- **World Health Organization Recommendations:** The World Health Organization (WHO) recommends an **annual average** of $\leq 5 \mu\text{g/m}^3$ for PM2.5 concentrations to safeguard public health. Exceeding these levels may lead to increased health risks, making it imperative to monitor and control PM2.5 pollution.

The outcomes of this analysis will not only enhance our understanding of PM2.5 variability but also assist policymakers and environmental scientists in formulating targeted interventions to mitigate the impact of air pollution on public health and the environment.

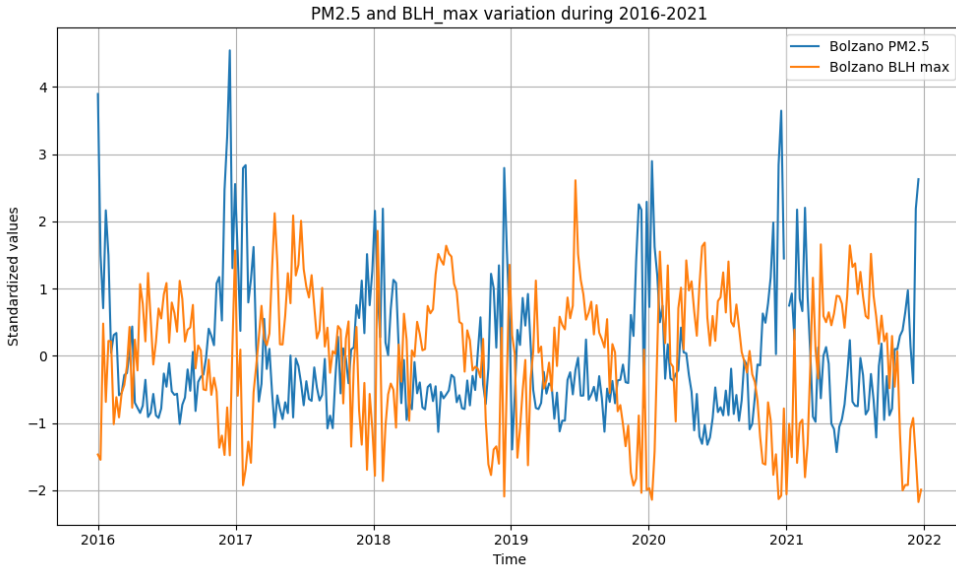


Figure 2: Correlation between PM2.5 Concentrations and Boundary Layer Height (BLH) max which represents the maximum depth of air next to the Earth's surface that is most affected by the resistance to the transfer of momentum, heat, or moisture across the surface.

3. Models

Regarding the choice of models, we first focused on three basic modeling approaches: spatial-informed partitioning of the data, covariate-informed partitioning and modeling temporal dependence in partitions. Each of the modeling methods is a hierarchical model with Gaussian likelihood, a Gaussian prior for cluster-specific means and an uniform prior for cluster-specific variances. All of them allow for a number of specifications, e.g. different setting ups of priors. Later, several extensions and combinations were considered.

In the whole section we denote by n the number of measurement units, by $\rho = \{S_1, \dots, S_k\}$ a partition of the n measurement units and by c_i the cluster that measurement unit i belongs to, i.e. $c_i = j$ if $i \in S_j$. Furthermore, cluster-specific values are marked with *. For example we consider cluster specific means $\boldsymbol{\mu}^* = \{\mu_1, \dots, \mu_k\}$ and standard deviations $\boldsymbol{\sigma}^*$.

3.1. sPPM Model: Spatial informed Clustering using location-dependent Similarity Functions

The following model is taken from [PQ16]. It is implemented as part of the R-package *ppmSuite* [Pag+23]. The overall model structure is the following, where $m \in \mathbb{R}, s^2 \in [0, \infty)$, the bounds $A, B \in [0, \infty)$ as well as the concentration parameter $M \in (0, \infty)$ and θ that will be explained in more detail below are user-defined parameters.

$$\begin{aligned} Y_i | \boldsymbol{\mu}^*, \boldsymbol{\sigma}^{2*}, c_i &\stackrel{\text{iid}}{\sim} \mathcal{N}(\mu_{c_i}^*, \sigma_{c_i}^{2*}), i = 1, \dots, n \\ (\mu_j^*, \sigma_j^*) | \mu_0, \sigma_0^2 &\stackrel{\text{iid}}{\sim} \mathcal{N}(\mu_0, \sigma_0^2) \times \text{UN}(0, A) \\ (\mu_0, \sigma_0) &\sim \mathcal{N}(m, s^2) \times \text{UN}(0, B) \\ \rho &\sim \text{sPPM}(M, \boldsymbol{\theta}) \end{aligned}$$

The *sPPM* is a prior of the following form, where \mathbf{s} denotes the spatial coordinates of the measurement units:

$$\mathbb{P}(\rho|\mathbf{s}) \propto \prod_{j=1}^{k_\rho} \left(\underbrace{M \cdot \Gamma(|S_j|)}_{=:c(S_j)} g(S_j, \mathbf{s}_j^* | \boldsymbol{\theta}) \right).$$

The so-called similarity function g is a non-negative function that measures the togetherness of the stations in the set S_j . Note that $\prod_{j=1}^{k_\rho} c(S_j)$ is proportional to the distribution of ρ in a random partition model induced by a sample from a Dirichlet process (Section 8.1.3 in [Gug23]). Therefore M takes the role of the concentration parameter in the Dirichlet process and influences the number of clusters.

For the similarity function g that incorporates the spatial information there are four options available.

1. $\theta = \alpha \in (0, \infty)$ with the distance measure

$$g_1(S_j, \mathbf{s}_j^* | \theta) := \begin{cases} \frac{1}{\Gamma(\alpha \mathcal{D}_h) \mathbf{1}[\mathcal{D}_h \geq 1] + \mathcal{D}_h \mathbf{1}[\mathcal{D}_h < 1]}, & \text{if } |S_h| > 1 \\ M, & \text{if } |S_h| = 1 \end{cases}$$

with a distance function $\mathcal{D}_h := \sum_{i \in S_h} d(\mathbf{s}_i, \bar{s}_h)$ and the cluster centroid $\bar{s}_{hk} = \frac{1}{n_h} \sum_{i \in S_h} s_{ik}$ for coordinates $k = 1, 2$ and $n_h := |S_h|$. Larger α favors denser clusters.

2. $\theta = a \in (0, \infty)$ with distance measure

$$g_2(S_h, \mathbf{s}_h^* | \theta) := \prod_{i,j \in S_h} \mathbf{1}[\|\mathbf{s}_i - \mathbf{s}_j\| \leq a].$$

Larger a allows for larger neighborhoods.

3. (*Auxiliary Cohesion*) With dimension $d = 2$ and $\boldsymbol{\xi} = (\mathbf{m}, \mathbf{V}) \in \mathbb{R}^d \times \mathbb{S}_+^d = \mathbb{R}^d \times \{X \in \mathbb{R}^{d \times d} | X \succeq 0\} =: \Xi$, we have (prior predictive conjugate model)

$$g_3(S_h, \mathbf{s}_h^* | \boldsymbol{\theta}) := \int_{\Xi} \prod_{i \in S_h} q(\mathbf{s}_i | \boldsymbol{\xi}_h) q(\boldsymbol{\xi}_h) d\boldsymbol{\xi}_h$$

with $q(\mathbf{s} | \boldsymbol{\xi}) = \mathcal{N}(\mathbf{s} | \boldsymbol{\xi})$ and $q(\boldsymbol{\xi}) = \text{NIW}(\mathbf{m}, \mathbf{V} | \boldsymbol{\mu}_0, \kappa_0, \nu_0, \Delta_0 \cdot \text{Id}_d)$ for user-defined parameters $\boldsymbol{\theta} = (\boldsymbol{\mu}_0, \kappa_0, \Delta_0, \nu_0) \in \mathbb{R}^d \times (0, \infty)^2 \times (1, \infty)$ (last part since $\nu_0 > d - 1$ has to be fulfilled)

4. (*Double Dipper*) With same structure as g_3 , but with a posterior predictive conjugate model

$$g_4(S_h, \mathbf{s}_h^* | \boldsymbol{\theta}) := \int_{\Xi} \prod_{i \in S_h} q(\mathbf{s}_i | \boldsymbol{\xi}_h) q(\boldsymbol{\xi}_h | \mathbf{s}_h^*) d\boldsymbol{\xi}_h$$

and conjugate model $q(\mathbf{s}_i | \boldsymbol{\xi}_h) = \mathcal{N}(\mathbf{s}_i | \mathbf{m}_h, \mathbf{V}_h)$ and $q(\boldsymbol{\xi}_h | \mathbf{s}_h^*) = \text{NIW}(\mathbf{m}_h, \mathbf{V}_h | \mathbf{s}_h^*)$ Compared to g_3 this option is more peaked and puts more weights on local partitions.

3.2. PPMx: Clustering using Covariate-dependent Similarity functions and Prior on Cluster Size

The covariate-informed partition model is taken from [PQ17] and all the introduced variants are implemented in the *R*-package `ppmSuite` [Pag+23]. The overall structure is the same as for the spatial-informed clustering with the difference that the similarity function now measures the homogeneity of the covariate values in a given partition set. Again, the values $m \in \mathbb{R}$, $s^2 \in [0, \infty)$ and bounds $A, B \in [0, \infty)$ as well as concentration parameter $M \in (0, \infty)$ and parameter(s) θ for the chosen similarity function are user-defined.

$$Y_i | \boldsymbol{\mu}^*, \boldsymbol{\sigma}^{2*}, c_i \stackrel{\text{ind}}{\sim} \mathcal{N}(\mu_{c_i}^*, \sigma_{c_i}^{2*}), i = 1, \dots, n$$

The prior for the clusters is

$$\mathbb{P}(\rho|\boldsymbol{x}) \propto \prod_{j=1}^{k_\rho} c(|S_j|) g(\boldsymbol{x}_j^*|\boldsymbol{\theta}).$$

For the so-called cohesion function c either the same function as in Section 3.1 (that is proportional to the partition probabilities in a random partition model derived from a Dirichlet process), or a uniform cohesion $c \equiv 1$ can be chosen.

In the following discussion $p = 1$ is assumed if not stated otherwise. If p covariates are available, in general

$$\tilde{g}(\boldsymbol{x}_j^*|\boldsymbol{\theta}) = \prod_{l=1}^p g(\boldsymbol{x}_{jl}^*|\boldsymbol{\theta})$$

is adopted.

As a large number of covariates can lead to either a large number of singleton clusters or one single cluster, there are two optional methods to cap the influence of the covariates on the partitioning.

$$(1) \quad \tilde{g}(\boldsymbol{x}_j^*) = \frac{g(\boldsymbol{x}_j^*)}{\sum_{i=1}^{k_j} g(\boldsymbol{x}_i^*)} \quad \text{or} \quad (2) \quad \tilde{g}(\boldsymbol{x}_j^*) = g(\boldsymbol{x}_j^*)^{\frac{1}{p}}$$

For similarity functions g there are four options available.

1. With $\theta = \alpha \in (0, \infty)$

$$g_1(\boldsymbol{x}_j^*|\theta) := \exp\{-\alpha H(\boldsymbol{x}_j^*)\}.$$

For continuous covariates $H(\boldsymbol{x}_j^*) = \frac{1}{n} \sum_{l \in S_j} (x_{jl} - \bar{x}_j)^2$ and for categorical covariates $H(\boldsymbol{x}_j^*) = \sum_{c=1}^C \hat{p}_{cj} \log \hat{p}_{cj}$, where C is the number of categories and \hat{p}_{cj} the proportion of observations in category c in cluster j . Higher values of α lead to an increased penalty for dissimilar covariate values. Extensions to the multivariate case are possible (determinant of cluster-specific covariate matrices or multivariate entropy respectively).

2. For any number of covariates p and penalty $\theta = \alpha \in (0, \infty)$

$$g_2(\boldsymbol{x}_j^*|\theta) := \exp\left\{-\alpha \sum_{i,k \in S_j, i \neq k} d(\boldsymbol{x}_i, \boldsymbol{x}_k)\right\}$$

and

$$g_3(\boldsymbol{x}_j^*|\theta) := \exp\left\{-\frac{2\alpha}{n_j(n_j-1)} \sum_{i,k \in S_j, i \neq k} d(\boldsymbol{x}_i, \boldsymbol{x}_k)\right\}$$

are based on the Gower Dissimilarity:

$$d(x_{il}, x_{jl}) := \begin{cases} \frac{|x_{il} - x_{jl}|}{\max_h x_{hl} - \min_h x_{hl}}, & \text{if } l\text{-th cov. continuous} \\ \delta_{x_{il} x_{jl}}, & \text{if } l\text{-th cov. categorical} \end{cases}$$

and $d(\boldsymbol{x}_i, \boldsymbol{x}_k)$ is the average of the Gower Dissimilarities in the p components.

3. (*Auxiliary Similarity Function*) With an auxiliary parameter ξ_j^* , we have (prior predictive conjugate model)

$$g_4(\boldsymbol{x}_j^*|\boldsymbol{\theta}) := \int \prod_{i \in S_j} q(x_i|\xi_j^*) q(\xi_j^*) d\xi_j^*$$

For continuous covariates there are two options as a conjugate model. First, the *Auxiliary N-N Model* with $q(\cdot|\xi_j^*) = \mathcal{N}(\cdot|\xi_j^*, \kappa_1 \hat{S})$ and $q(\xi_j^*) = \mathcal{N}(\xi_j^*|m_0, s_0^2)$ where \hat{S} denotes the empirical variance of the covariate. The user-supplied parameters are $\boldsymbol{\theta} = (\kappa_1, m_0, s_0)$. Second, the

Auxiliary N-NIG Model with $q(\cdot|\boldsymbol{\xi}_j^*) = \mathcal{N}(\cdot|m_j^*, v_j^*)$ and $q(\boldsymbol{\xi}_j^*) = \text{N-IG}(m_j^*, v_j^*|m_0, k_0, v_0, n_0)$. The user-supplied parameters are $\boldsymbol{\theta} = (m_0, k_0, v_0, n_0)$.

For categorical covariates a Multinomial-Dirichlet Model is applied, that is $q(\cdot|\boldsymbol{\xi}_j^*) = \text{Multinomial}(\cdot|\boldsymbol{\xi}_j^*)$ and $q(\boldsymbol{\xi}_j^*) = \text{Dirichlet}_{k_j}(\boldsymbol{\xi}_j^*|\boldsymbol{\alpha} \equiv a)$. The user-supplied parameter is $\theta = a$.

4. (*Double Dipper*) With an auxiliary parameter $\boldsymbol{\xi}_j^*$, we have

$$g_5(\mathbf{x}_j^*|\boldsymbol{\theta}) := \int \prod_{i \in S_j} q(x_i|\boldsymbol{\xi}_j^*) q(\boldsymbol{\xi}_j^*|\mathbf{x}_j^*) d\boldsymbol{\xi}_j^*$$

with the same options for the underlying models as for g_4 . This option gives more weight on the local covariate structure compared to g_4 .

3.3. DRPM Model: Dependent Modeling of Temporal Sequences of Random Partitions

In this model that is taken from [PQD21] and is implemented in the *R*-package `drpm` [Pag] finally a temporal evolvement of the partitions is considered. The overall model structure is the following:

$$\begin{aligned} Y_{it} | \boldsymbol{\mu}_t^*, \boldsymbol{\sigma}_t^{2*}, \mathbf{c}_t &\stackrel{\text{ind}}{\sim} \mathcal{N}(\mu_{c_{it}t}^*, \sigma_{c_{it}t}^{2*}) \quad \forall i = 1, \dots, n; t = 1, \dots, T \\ (\mu_{jt}^*, \sigma_{jt}^*) | \theta_t, \tau_t^2 &\stackrel{\text{ind}}{\sim} \mathcal{N}(\theta_t, \tau_t^2) \times \text{UN}(0, A_\sigma) \quad \forall j = 1, \dots, k_t \\ (\theta_t, \tau_t) &\stackrel{\text{iid}}{\sim} \mathcal{N}(\phi_0, \lambda^2) \times \text{UN}(0, A_\tau) \quad \forall t = 1, \dots, T \\ (\phi_0, \lambda) &\sim \mathcal{N}(m_0, s_0^2) \times \text{UN}(0, A_\lambda) \\ \{\mathbf{c}_1, \dots, \mathbf{c}_T\} &\sim \text{tRPM}(\boldsymbol{\alpha}, M) \text{ with } \alpha_t \stackrel{\text{iid}}{\sim} \text{Beta}(a_\alpha, b_\alpha). \end{aligned}$$

The temporal random partition model models the temporal sequence of clusters as a first-order Markovian structure. We denote the clusters as $\rho_t = \{S_{1t}, \dots, S_{k_t t}\}$, $t = 1, \dots, T$ or use the cluster-labeling notation.

The first ingredient for the model is an exchangeable probability function (EPPF) on the set of partitions of the measurement units. In our case

$$P(\rho|M) = \frac{M^{k_\rho}}{\prod_{i=1}^n (M+i-1)} \prod_{i=1}^{k_\rho} (|S_i|-1)!$$

is applied. This is the marginal probability function for ρ derived from a Chinese Restaurant process with concentration parameter M . Smaller M favors less but larger clusters. This function is the prior for ρ_1 .

Secondly, in order to define transition probabilities an auxiliary parameter γ_t is introduced. We define $\gamma_{it} \sim \text{Ber}(\alpha_t)$, i.e. $\gamma_t \in \{0, 1\}^{\#\text{stations}}$ and give the following interpretation:

$$\gamma_{it} = \begin{cases} 1, & \text{station } i \text{ is \textbf{not} relocated when moving from time } t-1 \text{ to } t \\ 0, & \text{else} \end{cases}.$$

The values of $\alpha_t \in [0, 1]$ regulate the time-dependency, e.g. $\alpha_t = 1$ means $\rho_t = \rho_{t-1}$ with probability 1 and $\alpha_t = 0$ implies ρ_t is independent of ρ_{t-1} .

Given γ_t and ρ_{t-1} there is restriction to what partitions are compatible and can be considered for ρ_t . The transition probabilities are then

$$\mathbb{P}(\gamma_1, \rho_1, \dots, \gamma_T, \rho_T) = \mathbb{P}(\rho_T | \gamma_T, \rho_{T-1}) \cdots \mathbb{P}(\rho_2 | \gamma_2, \rho_1) \mathbb{P}(\rho_1)$$

and for $t \in \{1, \dots, T\}$ the $\mathbb{P}(\rho_t | \gamma_t, \rho_{t-1})$ is given by the chosen EPPF from before truncated to the set of compatible partitions.

3.4. Extensions

DPRM Model:

- Spatial data
- AR(1)-method using eta not equal to zero (otherwise iid)
- unit, i.e. station, specific alpha values – adjust the prior size accordingly
- fixed α for each time step
- phi value, 0 value corresponds to independent atoms

4. Data Preparation and Evaluation

4.1. The Agrimonia Database

4.2. Data Exploration

TODO: show the correlation plot, show time series over different years list data loss, number of stations

4.3. Imputation of Missing Data

4.4. Data Aggregation

4.5. Evaluation

4.5.1 Goodness-of-fit

To indicate goodness-of-fit of the used models the following criteria are considered.

- LPML = log pseudo marginal likelihood (higher is better)

The LPML is a predictive information criterion based on the idea of leave-one-out cross validation [Gug23]. Let $\mathbf{y} = (y_1, \dots, y_n)$ denote our data, $\mathbf{y}_{(-i)} = (y_1, \dots, y_{i-1}, y_{i+1}, \dots, y_n)$ and $m(y_i|\mathbf{y}_{(-i)})$ the marginal likelihood of y_i given $\mathbf{y}_{(-i)}$ in the considered model. Then the LPML is defined as

$$\text{LPML} = \sum_{i=1}^n \log m(y_i|\mathbf{y}_{(-i)}).$$

- WAIC = widely applicable information criterion (lower is better)

The WAIC is another predictive information criterion that accounts for the over-estimation of log pointwise predictive density $\sum_{i=1}^n \log m(y_i|\mathbf{y})$ by subtracting a penalization term p_{WAIC} [Gug23]. In our definition the WAIC is obtained by multiplying this difference with -2 . In the following θ denotes the parameters and f the likelihood of the given model. The WAIC is defined as

$$\begin{aligned} \text{WAIC} &= -2 \left(\sum_{i=1}^n \log m(y_i|\mathbf{y}) - p_{\text{WAIC}} \right), \\ p_{\text{WAIC}} &= \sum_{i=1}^n \text{Var}_{\theta|\mathbf{y}} \log f(y_i|\theta). \end{aligned}$$

- MSE = mean squared error (lower is better)

Denote by $\hat{y}_i = \mathbb{E}(Y_i|\mathbf{y})$ the posterior mean of the i -th observation, then

$$\text{MSE} = \frac{1}{n} \sum_{i=1}^n (y_i - \hat{y}_i)^2.$$

- MaxDev (lower is better): Given a partition $\rho = \{S_1, \dots, S_k\}$ we compute the maximum of

the cluster-internal deviation of PM2.5 values over all cluster, namely

$$\text{MaxDev} = \max_{i=1,\dots,k} \left(\max_{i \in S_k} y_i - \min_{i \in S_k} y_i \right)$$

as an indication on how closely related the target variable's values are given the partition ρ .

4.5.2 Predictive Performance

The predictive performance of the models is measured by the mean squared prediction error.

- MSPE = mean squared prediction error (lower is better)

Denote by \tilde{y}_i the testing observation for the i -th measurement unit, then

$$\text{MSPE} = \frac{1}{n} \sum_{i=1}^n (\tilde{y}_i - \hat{y}_i)^2.$$

4.5.3 Cluster estimation

Once a model is fit to the data the question remains how to summarize the obtained posterior for the clusters in a meaningful way. One number that we report is the posterior mean of the number of clusters. Furthermore, a general idea is to find an estimate $\hat{\rho}^*$ that minimizes a certain partition loss function L . Assuming that there is a “true” ρ (we take the posterior distribution), this becomes

$$\hat{\rho}^* = \operatorname{argmin}_{\hat{\rho}} \mathbb{E}(L(\rho, \hat{\rho}) | \mathbf{y}) \approx \frac{1}{M} \sum_{m=1}^M L(\rho^{(m)}, \hat{\rho}),$$

where $(\rho^{(1)}, \dots, \rho^{(M)})$ are MCMC samples from the posterior. For that approach the *R*-package **salso** [DJa23] provides a number of possibilities. In [DJM22] different loss functions are explained as well as the **SALSO** algorithm that is implemented in the package.

Binder Loss

One of the most widely used loss functions is the Binder loss function that considers pairwise misclassifications. Switching to the equivalent cluster notation for partitions the definition is

$$L_{\text{Binder}}(\mathbf{c}, \hat{\mathbf{c}}) = \sum_{i < j} a \cdot I(\{c_i = c_j\})I(\{\hat{c}_i \neq \hat{c}_j\}) + b \cdot I(\{c_i \neq c_j\})I(\{\hat{c}_i = \hat{c}_j\}).$$

For $a = b = 1$ a measure of similarity between partitions, the Rand Index, is obtained by $\text{RI}(\rho, \hat{\rho}) = 1 - L_{\text{Binder}}(\rho, \hat{\rho}) / \binom{n}{2}$. Maximizing the the posterior expectation of the Rand Index is equivalent to minimizing the expected loss for a Binder loss function with $a = b = 1$. As this index fails to account for chance agreements, there exists a generalization that we will consider.

Adjusted Rand Index

The Adjusted Rand Index (ARI) is defined as

$$\text{ARI}(\rho, \hat{\rho}) = \frac{\sum_{S \in \rho} \sum_{E \in \hat{\rho}} \binom{|S \cap E|}{2} - \left(\sum_{S \in \rho} \binom{|S|}{2} \sum_{E \in \hat{\rho}} \binom{|E|}{2} \right) \frac{1}{\binom{n}{2}}}{\frac{1}{2} \left(\sum_{S \in \rho} \binom{|S|}{2} + \sum_{E \in \hat{\rho}} \binom{|E|}{2} \right) - \left(\sum_{S \in \rho} \binom{|S|}{2} \sum_{E \in \hat{\rho}} \binom{|E|}{2} \right) \frac{1}{\binom{n}{2}}}.$$

Large values mean a larger similarity between the partitions. We obtain another point estimate of the posterior expectation of the partition by maximizing the posterior expectation of the ARI.

5. Results

We used the same seed for every experiments to make the results reproducible and comparable

5.1. sPPM

5.2. PPMx

5.3. DRPM

TODO

- Analyse large experiment
- Analyse Extension of large Experiment

Name \ Prior Parameters	m_0	s_0^2	A_σ	A_r	A_λ	b	a_α	b_α
DRPM-Paper [PQD21]	0.0	100^2	10.0	5.0	5.0	1.0	2.0	2.0
Lower Std (ours)	0.0	200	0.1	1.0	1.0	1.0	1.0	1.0
Mean 2018 (ours)	2.91	200	0.1	1.0	1.0	1.0	1.0	1.0

Table 1: Different Prior Parameters for the three models we used for our initial large test.

5.4. Extensions

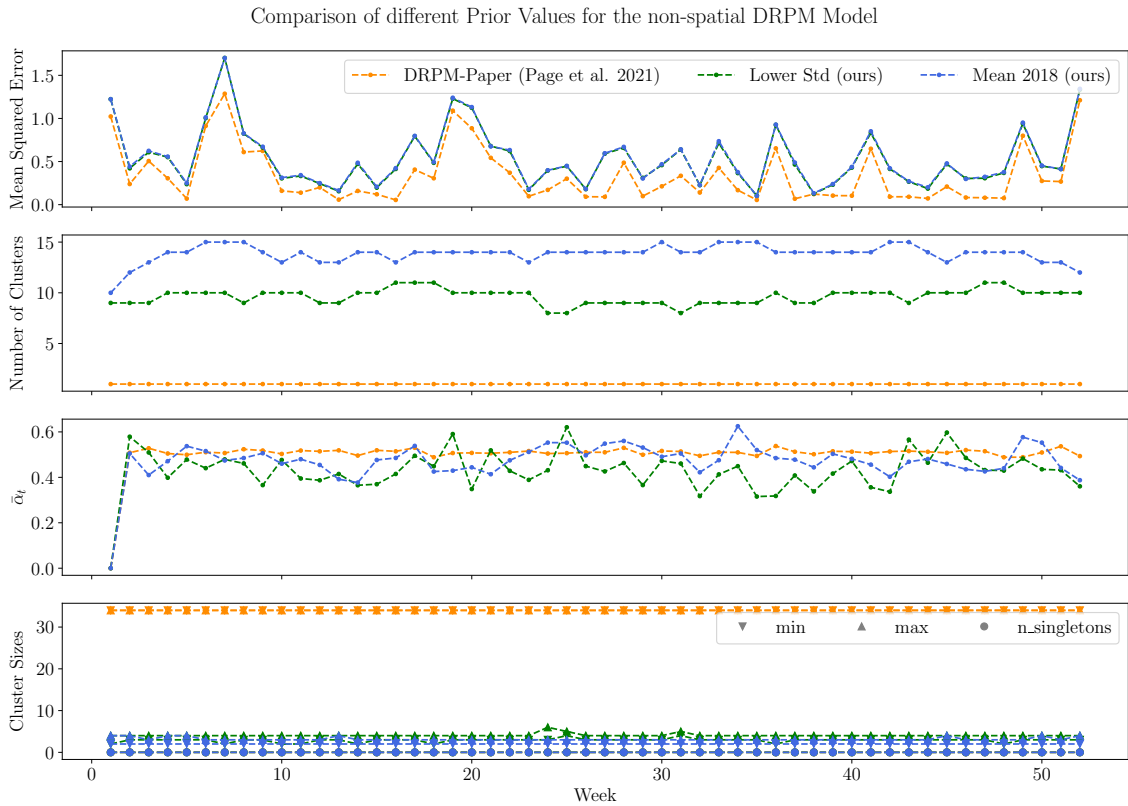


Figure 3: Comparison of the best model for each prior for DRPM without spatial cohesion. The used prior values are listed in table 1. For the DRPM model itself we use $M = 0.1$ as the concentration parameter. The MCMC uses 10000 draws with a burn of 1000 and a thinning of 10, resulting in 900 total MCMC samples. The DRPM-Paper model reached a WAIC (lower is better) of $3.103 \cdot 10^{+03}$ while our models achieved a WAIC score of $-1.285 \cdot 10^{+03}$ and $-9.548 \cdot 10^{+02}$ for the Lower Std and Mean 2018 models respectively.

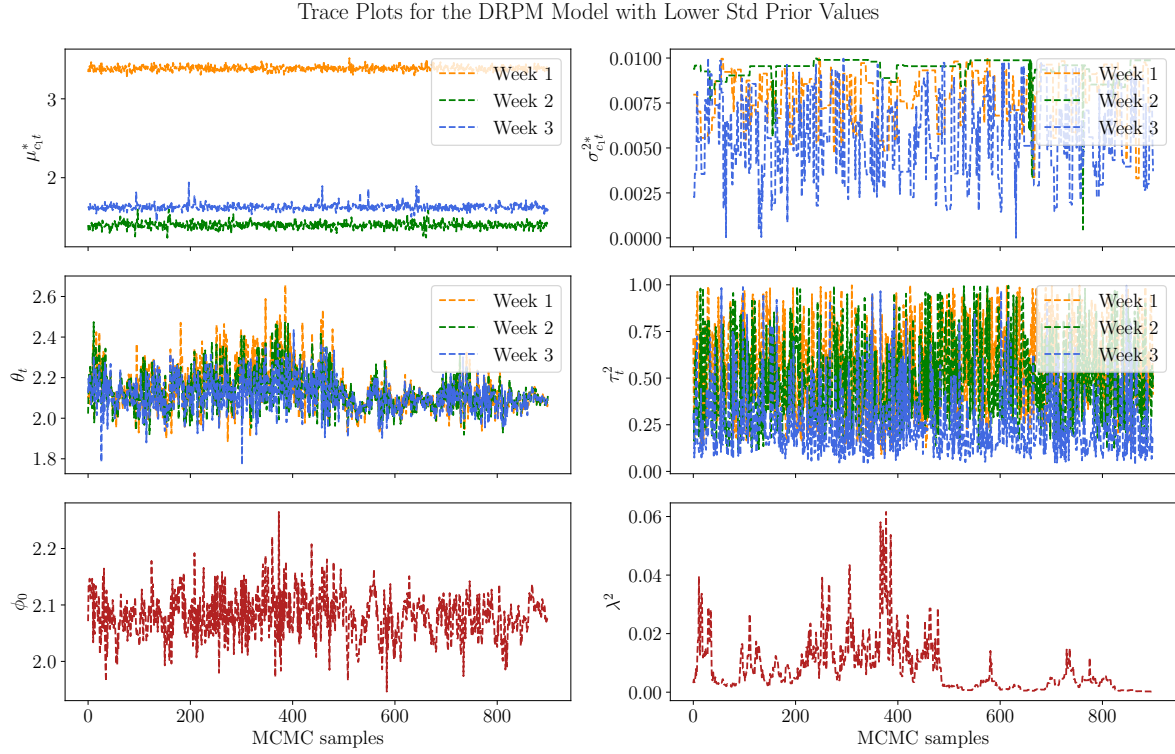


Figure 4: Trace Plots for the DRPM Model parameters with the Lower Std Prior values. Week specific parameters are shown for the first three weeks of the year and cluster specific parameters are presented for the first cluster.

6. Conclusions

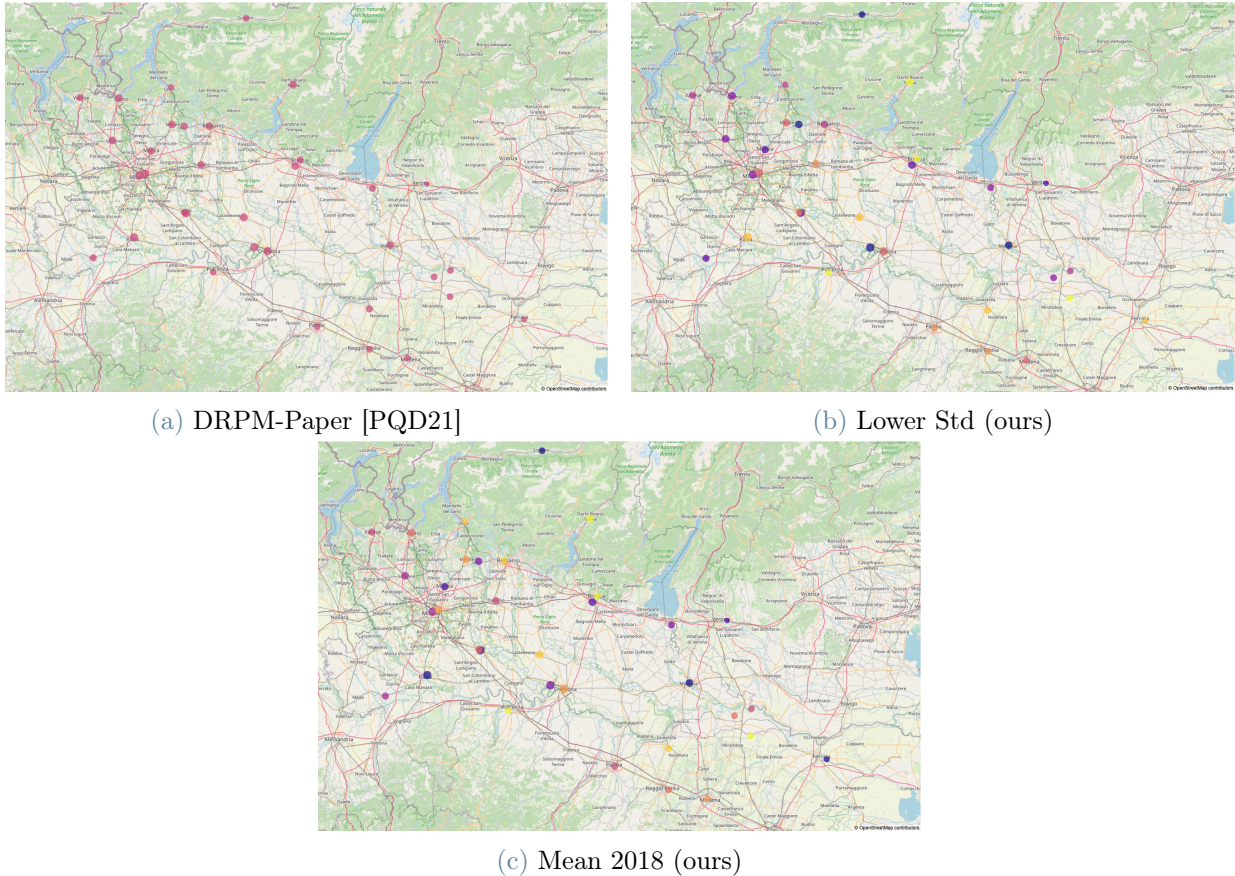


Figure 5: Exemplary clustering for week three of the year 2019 using all three of our base models without spatial information. All use the concentration parameter $M = 0.1$ and the prior parameters listed in table 1. The color of the bubble indicates the cluster and the size of the bubble the average PM2.5 value within week three of 2018.

References

- [DJa23] David B. Dahl, Devin J Johnson, and et al. *Package 'salso': Search Algorithms and Loss Functions for Bayesian Clustering*. version 0.3.35. 2023. URL: <https://github.com/dbdahl/salso>.
- [DJM22] David B. Dahl, Devin J. Johnson, and Peter Müller. “Search Algorithms and Loss Functions for Bayesian Clustering”. In: *Journal of Computational and Graphical Statistics* 31.4 (2022), pp. 1189–1201. DOI: 10.1080/10618600.2022.2069779. eprint: <https://doi.org/10.1080/10618600.2022.2069779>. URL: <https://doi.org/10.1080/10618600.2022.2069779>.
- [Gug23] Alessandra Guglielmi. *Bayesian Statistics: Lecture Notes*. 2023.
- [MQR11] Peter Müller, Fernando A Quintana, and Gary L. Rosner. “A Product Partition Model With Regression on Covariates”. In: *Journal of Computational and Graphical Statistics* 20.1 (2011). PMID: 21566678, pp. 260–278. DOI: 10.1198/jcgs.2011.09066. eprint: <https://doi.org/10.1198/jcgs.2011.09066>. URL: <https://doi.org/10.1198/jcgs.2011.09066>.
- [Pag] Garrett L. Page. *Package 'drpm': Dependent Random Partition Model*. version 0.1.2. URL: <https://github.com/gpage2990/drpm>.
- [Pag+23] Garrett L. Page et al. *Package 'ppmSuite': A Collection of Models that Employ Product Partition Distributions as a Prior on Partitions*. version 0.3.4. 2023. URL: <https://cran.r-project.org/web/packages/ppmSuite/index.html>.
- [PQ16] Garrett L. Page and Fernando A. Quintana. “Spatial Product Partition Models”. In: *Bayesian Analysis* 11.1 (2016), pp. 265–298. DOI: 10.1214/15-BA971. URL: <https://doi.org/10.1214/15-BA971>.
- [PQ17] Garrett L. Page and Fernando A. Quintana. “Calibrating covariate informed product partition models”. In: *Statistics and Computing* 28 (2017), pp. 1009–1031. DOI: 10.1007/s11222-017-9777-z. URL: <https://doi.org/10.1007/s11222-017-9777-z>.
- [PQD21] Garrett L. Page, Fernando A. Quintana, and David B. Dahl. *Dependent Modeling of Temporal Sequences of Random Partitions*. 2021. arXiv: 1912.11542 [stat.ME].
- [PQD22] Garrett L. Page, Fernando A. Quintana, and David B. Dahl. “Spatio-Temporal Random Partition Models”. In: (2022). URL: <https://arxiv.org/pdf/1912.11542v1.pdf>.
- [R C23] R Core Team. *R: A Language and Environment for Statistical Computing*. R Foundation for Statistical Computing. Vienna, Austria, 2023. URL: <https://www.R-project.org/>.
- [RLJ21] G.L. Rosner, P.W. Laud, and W.O. Johnson. *Bayesian Thinking in Biostatistics*. 1st edition. Chapman and Hall/CRC, 2021. URL: <https://doi.org/10.1201/9781439800102>.
- [Rod+23] Alessandro Fassò Jacopo Rodeschini et al. “Agrimonia: a dataset on livestock, meteorology and air quality in the Lombardy region, Italy”. In: *Scientific Data* 10.1 (Mar. 2023). ISSN: 2052-4463. DOI: 10.1038/s41597-023-02034-0. URL: <http://dx.doi.org/10.1038/s41597-023-02034-0>.

7. Acknowledgements